

Numerical approximation for a nonlinear membrane problem

Hervé Le Dret, Nabil Kerdid, Abdelkader Saïdi

► **To cite this version:**

Hervé Le Dret, Nabil Kerdid, Abdelkader Saïdi. Numerical approximation for a nonlinear membrane problem. 2006. <hal-00112123>

HAL Id: hal-00112123

<https://hal.archives-ouvertes.fr/hal-00112123>

Submitted on 8 Nov 2006

HAL is a multi-disciplinary open access archive for the deposit and dissemination of scientific research documents, whether they are published or not. The documents may come from teaching and research institutions in France or abroad, or from public or private research centers.

L'archive ouverte pluridisciplinaire **HAL**, est destinée au dépôt et à la diffusion de documents scientifiques de niveau recherche, publiés ou non, émanant des établissements d'enseignement et de recherche français ou étrangers, des laboratoires publics ou privés.

Numerical approximation for a nonlinear membrane problem

Nabil Kerdid* Hervé Le Dret[†] Abdelkader Saïdi[‡]

September 12, 2006

Abstract

We present a numerical study of large deformations of nonlinearly elastic membranes. We consider the nonlinear membrane model obtained by H. Le Dret and A. Raoult using Γ -convergence, in the case of a Saint Venant-Kirchhoff bulk material. We consider conforming P_1 and Q_1 finite element approximations of the membrane problem and use a nonlinear conjugate gradient algorithm to minimize the discrete energy. We present numerical tests including membranes submitted to live pressure loads.

1 Introduction

The purpose of this article is to devise numerical approximations of large deformations of a nonlinearly elastic membrane. The nonlinear membrane model used here was obtained in [6], with refinements in [9]. The relevance of this model stems from the fact that it was derived from three-dimensional nonlinear elasticity by means of a rigorous convergence method. Our numerical study of the nonlinear membrane model is made possible due to the explicit formula for the nonlinear membrane energy given in [6] in the case of the Saint Venant-Kirchhoff bulk material. For a general bulk material, an explicit computation of the corresponding nonlinear membrane energy entails the determination of the quasiconvex envelope

*College of Computer and Information Sciences, Imam University, Riyadh, Saudi Arabia.
Email: nkerdid@ccis.imamu.edu.sa

[†]Université Pierre et Marie Curie-Paris6, UMR 7598 LJLL, Paris, F-75005 France ; CNRS, UMR 7598 LJLL, Paris, F-75005 France. Email: ledret@ccr.jussieu.fr

[‡]Institut de Recherche Mathématique Avancée, Université Louis Pasteur, 7 rue René Descartes, 67084 Strasbourg, France. Email: saidi@math.u-strasbg.fr

of a function defined on the space of 3×2 matrices, a hopeless task as a general rule.

This article is organized as follows: We first briefly present the results of [6] and [9]. We consider a three-dimensional hyperelastic homogeneous cylinder of thickness $2\varepsilon > 0$ made of a given Saint Venant-Kirchhoff material. The body is submitted to a dead loading body force density and a constant pressure differential on its upper and lower surfaces, and a boundary condition of place on its lateral surface. The three-dimensional nonlinear elasticity equilibrium problem is formulated as a minimization problem for the total energy of the body.

Using Γ -convergence arguments, H. Le Dret and A. Raoult showed that deformations that almost minimize the three-dimensional total energy converge when the thickness ε of the body goes to zero towards deformations that minimize a nonlinear membrane energy, see [6]. The convergence takes place in a rescaled weak $W^{1,p}$ sense. The limit problem is two-dimensional, with values in \mathbb{R}^3 .

The limit two-dimensional nonlinear membrane energy is computed in two steps: First minimize the bulk stored energy function with respect to the third column vector of the deformation gradient—this step produces a function W_0 on the space of 3×2 matrices—then take the quasiconvex envelope of W_0 . In the special case of a Saint Venant-Kirchhoff material, an explicit formula for this quasiconvex envelope QW_0 is available. This formula is expressed in terms of the right singular values of the membrane deformation. In [9], in addition to the case of curved membranes, the zero-thickness limit of a constant live pressure loading term is also computed.

In section 3, we present a conforming finite element approximation of the membrane problem. We consider P_1 and Q_1 discretizations of the three Cartesian components of the deformation. We prove the weak- $W^{1,4}$ convergence of the approximate solutions toward a solution of the continuous minimization problem.

The choice of available numerical methods to solve our FE problem is rather limited since the problem under study is highly nonlinear and the membrane stored energy function is only of class C^1 . Consequently, a method relying on second derivatives of the total energy cannot be appropriate. On the contrary, the nonlinear conjugate gradient method with the Polak and Ribière variant seems to be well adapted to our problem. The convergence of the algorithm is guaranteed by the convexity of the membrane energy, at least in the case of zero pressure differential. There is however a difficulty in computing the gradient of the stored energy function. We adapted Ball's results concerning the differentiability of frame-indifferent, isotropic functions on the space of $n \times n$ square matrices, see [2].

In section 4, we present various numerical tests. Both P_1 and Q_1 elements are alternatively used. The first test is a circular membrane submitted to an upward pressure differential and clamped on its boundary. It should be noted that in our formulation, there is absolutely no need to track the deformed normal vector in

order to take into account the live loading pressure differential. This is exemplified by the bubble-like deformation computed in this test.

Next, we perform a few tests taken from [12]: a rectangular airbag and a square membrane attached by its four corners and submitted to a vertical point force applied at its center. As opposed to [12], our model cannot capture wrinkles in detail, because wrinkles are filtered out in the Γ -limit process, which in turn leads to a well-posed limit minimization problem. Such is the nature of weak convergence. However, wrinkled regions are captured. They are the membrane areas where the deformation gradient lies a region of 3×2 space where relaxation occurs, *i.e.*, the quasiconvex envelope is such that $QW_0 < W_0$. This occurs in compression when at least one of the singular values is less than 1 and the other one is not too large, see [6] for details.

The last two tests are in the context of the modeling of fabrics. The first test is a square piece of fabric attached at its center and submitted to a vertical dead loading body force and the second is a tablecloth with no displacement allowed on the table surface.

Part of the results of this article were announced in [5].

2 The continuous problem

Let us briefly outline the results of [6] and [9], to which we refer the reader for more details. Let ω be an open, bounded subset of \mathbb{R}^2 with Lipschitz boundary. For all $\varepsilon > 0$, we consider a hyperelastic homogeneous body occupying the reference configuration $\Omega_\varepsilon = \omega \times]-\varepsilon, \varepsilon[$. We assume that the stored energy function of this body is a function $W: \mathbb{M}_3 \rightarrow \mathbb{R}$ which is continuous, coercive and satisfies growth conditions for an exponent $p \in]3, +\infty[$, where \mathbb{M}_3 is the space of real 3×3 matrices. We furthermore assume that the body is submitted to a dead loading body force density f and to a constant pressure differential $\varepsilon\Delta p$ on its upper and lower surfaces, which is a live load, that is to say a spatially constant pressure p_ε^+ on the upper surface and another spatially constant pressure p_ε^- on the lower surface such that $p_\varepsilon^+ - p_\varepsilon^- = \varepsilon\Delta p$. The equilibrium problem for this body may be formulated as a minimization problem for the energy

$$J_\varepsilon(\phi) = \int_{\Omega_\varepsilon} W(\nabla\phi) dx - \int_{\Omega_\varepsilon} f_\varepsilon \cdot \phi dx - P_\varepsilon(\phi), \quad (1)$$

where

$$P_\varepsilon(\phi) = \int_{\Omega_\varepsilon} \left[\pi_\varepsilon \det \nabla\phi + \frac{1}{3} \nabla\pi_\varepsilon \cdot (\text{cof} \nabla\phi^T \phi) \right] dx, \quad (2)$$

over a set of admissible deformations ϕ belonging to an appropriate Sobolev space and satisfying given boundary conditions of place on part of the lateral boundary.

Here, π_ε is a C^1 -function on $\bar{\Omega}_\varepsilon$ that takes the values p_ε^\pm on the upper and lower surfaces. The term P_ε appearing in the energy accounts for the pressure load, see [1]. Note that this term incorporates the fact that a pressure load is a live load that follows the normal vector to the deformed body, without having to keep track of this normal vector. Dead loading tractions on the upper, lower and lateral surfaces can also easily be added as well as boundary conditions of place on part of the boundary.

In [6] and [9], see the latter for the pressure term, Le Dret and Raoult proved that a rescaled version of the above three-dimensional energy Γ -converges when the thickness 2ε of the membrane goes to zero in the sense of the weak topology of $W^{1,p}(\Omega; \mathbb{R}^3)$, thereby showing that minimizing deformations converge, in an appropriate sense, toward solutions of a two-dimensional minimization problem. The limit, two-dimensional nonlinear membrane problem is described as follows.

Let $\mathbb{M}_{3,2}$ be the space of real 3×2 matrices. If $z_\alpha, \alpha = 1, 2$, are two vectors in \mathbb{R}^3 , we note $(z_1|z_2)$ the matrix of $\mathbb{M}_{3,2}$ whose columns are the vectors z_α . For all $F = (z_1|z_2) \in \mathbb{M}_{3,2}$ and $z \in \mathbb{R}^3$, we note $(F|z)$ the matrix whose first two columns are z_α , and third column is z and write $(z|F)$ with a similar convention. We now define a function $W_0: \mathbb{M}_{3,2} \rightarrow \mathbb{R}$ by

$$W_0(F) = \inf_{z \in \mathbb{R}^3} W((F|z)). \quad (3)$$

The function W_0 is continuous and coercive. Let QW_0 be its quasiconvex envelope, see [3]. We introduce the space of admissible membrane displacements

$$\Phi_M = \{ \psi \in W^{1,p}(\omega; \mathbb{R}^3); \psi(x_1, x_2) = (x_1, x_2, 0)^T \text{ on } \partial\omega \}, \quad (4)$$

(this is for the case of a boundary condition of place on the whole lateral surface $\partial\omega \times]-\varepsilon, \varepsilon[$ in the 3D problem, other conditions are enforced accordingly).

The limit nonlinear membrane energy is then defined by

$$J(\psi) = 2 \int_\omega QW_0(\nabla \psi) dx_1 dx_2 - \int_\omega f \cdot \psi dx_1 dx_2 - \frac{\Delta p}{3} \int_\omega \det(\partial_1 \psi | \partial_2 \psi | \psi) dx_1 dx_2, \quad (5)$$

for all $\psi \in \Phi_M$, where f is a 2D-body force resultant density obtained from f_ε .

The limit minimization problem now reads: Find $\varphi \in \Phi_M$ such that

$$J(\varphi) = \inf_{\psi \in \Phi_M} J(\psi). \quad (6)$$

The energy functional J is obtained via a Γ -limit process and existence of a solution to problem (6) is guaranteed under reasonable technical assumptions, see [6] and [9].

In general, it is not possible to compute explicitly the quasiconvex envelope of a given function W_0 . Hence, generically with respect to the bulk material, it

is not possible to perform numerical computations using this model. However, in the special case of a Saint Venant-Kirchhoff material, the quasiconvex envelope QW_0 was computed in [6]. Let us recall that the stored energy function of a Saint Venant-Kirchhoff material assumes the form

$$W(F) = \frac{\mu}{4} \operatorname{tr}((F^T F - I_3)^2) + \frac{\lambda}{8} (\operatorname{tr}(F^T F - I_3))^2,$$

where $\mu > 0$ and $\lambda \geq 0$ are the Lamé constants of the material (here F is a 3×3 matrix and I_n is the $n \times n$ identity matrix). The intermediate function W_0 is given by

$$\begin{aligned} W_0(F) = \frac{\mu}{4} \operatorname{tr}((F^T F - I_2)^2) + \frac{\lambda \mu}{4(\lambda + 2\mu)} h(F)^2 \\ + \frac{1}{8(\lambda + 2\mu)} ([\lambda h(F) - (\lambda + 2\mu)]_+)^2, \end{aligned}$$

with $h(F) = \operatorname{tr}(F^T F - I_2)$ (here F is a 3×2 matrix, thus $F^T F$ is 2×2) and t_+ denotes the positive part of t . Finally, the quasiconvex envelope QW_0 is expressed in terms of the right singular values $0 \leq v_1(F) \leq v_2(F)$ of F (i.e. the eigenvalues of $\sqrt{F^T F}$) as

$$\begin{aligned} QW_0(F) &= \Phi(v_1(F), v_2(F)) \\ &= \frac{E}{8} ([v_2(F)^2 - 1]_+)^2 + \frac{E}{8(1-v^2)} ([v_1(F)^2 + v v_2(F)^2 - (1+v)]_+)^2 \\ &\quad + \frac{E}{8(1-v^2)(1-2v)} ([v(v_1(F)^2 + v_2(F)^2) - (1+v)]_+)^2, \end{aligned} \quad (7)$$

where $E = \frac{\mu(3\lambda+2\mu)}{\lambda+\mu}$ is the Young modulus and $v = \frac{\lambda}{2(\mu+\lambda)}$ the Poisson ratio of the Saint Venant-Kirchhoff material under consideration, see [6] and [8]. It turns out that the function QW_0 is convex on $\mathbb{M}_{3,2}$, therefore the quasiconvex envelope of W_0 is also its convex envelope in this case.

In the case of the Saint Venant-Kirchhoff material, we thus have a completely explicit expression of the membrane energy that is rigorously derived from three-dimensional nonlinear elasticity by means of a convergence result. The pressure term

$$P(\psi) = \frac{\Delta p}{3} \int_{\omega} \det(\partial_1 \psi | \partial_2 \psi | \psi) dx_1 dx_2$$

also incorporates the fact that we are dealing with a live load that follows the normal to the deformed surface, see [9]. This feature is be very advantageous for numerical simulations since the deformed normal vector does not explicitly enter this formula. There thus is no need to recalculate this vector at each step of the approximation procedure, as opposed to [12] for example.

3 The discrete problem

3.1 Finite element discretization

We use P_1 and Q_1 discretizations. Let us describe the P_1 case since the Q_1 case is entirely similar at this stage. Let τ_h be a regular affine family of triangulations covering the domain ω . We discretize the three Cartesian components of the deformation using continuous P_1 finite elements. The discrete space of admissible displacements is given by

$$\Phi_M^h = \{ \psi_h \in C^0(\bar{\omega}; \mathbb{R}^3), \psi_h(x_1, x_2) = (x_1, x_2, 0)^T \text{ on } \partial\omega, \psi_h|_K \in (P_1)^3; \forall K \in \tau_h \}. \quad (8)$$

We clearly have $\Phi_M^h \subset \Phi_M$ and the approximation is conforming.

We approximate the continuous problem as follows: Find $\phi_h \in \Phi_M^h$ such that

$$J(\phi_h) = \inf_{\psi_h \in \Phi_M^h} J(\psi_h). \quad (9)$$

This is a convergent approximation scheme in the following sense.

Proposition 3.1 *The weak limit points of the sequence ϕ_h in $W^{1,4}$ are minimizers of problem (6).*

Proof. We first show that the functional J is sequentially weakly lower semicontinuous on $W^{1,4}(\omega; \mathbb{R}^3)$. The first two terms

$$J(\psi) - P(\psi) = 2 \int_{\omega} QW_0(\nabla\psi) dx_1 dx_2 - \int_{\omega} f \cdot \psi dx_1 dx_2$$

combine to form a convex, strongly continuous functional, hence weakly lower semicontinuous functional on $W^{1,4}(\omega; \mathbb{R}^3)$. For the pressure term, we observe that the components of the vector $\partial_1 \psi \wedge \partial_2 \psi$ are null Lagrangians. Since we are in dimension 2, it is well-known that the mapping $\psi \mapsto \partial_1 \psi \wedge \partial_2 \psi$ is sequentially weakly continuous from $W^{1,4}(\omega; \mathbb{R}^3)$ into $L^2(\omega; \mathbb{R}^3)$, see e.g. [1]. Let us take a weakly convergent sequence $\psi_k \rightharpoonup \psi$ in $W^{1,4}(\omega; \mathbb{R}^3)$. By Rellich's theorem, we have that $\psi_k \rightarrow \psi$ in $L^2(\omega; \mathbb{R}^3)$ and since $\det((u|v|w)) = (u \wedge v) \cdot w$, it clearly follows that

$$P(\psi_k) = \frac{\Delta p}{3} \int_{\omega} (\partial_1 \psi_k \wedge \partial_2 \psi_k) \cdot \psi_k dx_1 dx_2 \rightarrow P(\psi),$$

when $k \rightarrow +\infty$.

Since the functional J is coercive over Φ_M , it follows that the sequence ϕ_h is bounded. Let h' be a subsequence such that $\phi_{h'}$ converges weakly in $W^{1,4}(\omega; \mathbb{R}^3)$ to a limit point ϕ .

Let us now take $\psi \in \Phi_M$. Since the triangulation family is regular, there exists a sequence $\psi_{h'} \in \Phi_M^{h'}$ such that $\psi_{h'} \rightarrow \psi$ strongly in $W^{1,4}(\omega; \mathbb{R}^3)$. Therefore

$$J(\phi) \leq \liminf_{h' \rightarrow 0} J(\phi_{h'}) \leq \lim_{h' \rightarrow 0} J(\psi_{h'}) = J(\psi),$$

hence the result. \square

Remark 1 By the Rellich-Sobolev embeddings, we also have strong convergence in $C^{0,\alpha}(\bar{\omega}; \mathbb{R}^3)$ for all $\alpha < 1/2$. However, even if $\Delta p = 0$ and the functional J is convex, it is not strictly convex. Therefore, we cannot deduce strong $W^{1,4}$ convergence in general.

Note also that the above weak convergence holds true in $W^{1,p}$, not only for the Saint Venant-Kirchhoff material, but for a general material satisfying the hypotheses of [6] with $p > 3$, since quasiconvexity is sufficient to ensure the weak lower semicontinuity of the elastic term in the energy. Besides, the weak lower semicontinuity result can also essentially be viewed as a consequence of the Γ -convergence result. \square

3.2 The Polak-Ribière nonlinear conjugate gradient algorithm

The boundary value problem underlying problem (6) is highly nonlinear and so is its finite element counterpart. In order to perform numerical computations, we thus need a nonlinear method. The Newton method requires the Hessian of J on Φ_M^h , but the function QW_0 is not of class C^2 . Therefore, this method, or any method relying on second derivatives of J , is not appropriate. Furthermore, the problem is naturally set as an energy minimization problem. We thus use the nonlinear conjugate gradient method with the Polak and Ribière variant, see [10], which gives the best results. The conjugate gradient algorithm at the k th iteration is given by:

$$\begin{aligned} \psi_h^{k+1} &= \psi_h^k - \rho^k d^k, \\ d^k &= \nabla J(\psi_h^k) - \beta^{k-1} d^{k-1}, \\ \beta^k &= -\frac{[\nabla J(\psi_h^{k+1}) - \nabla J(\psi_h^k)] \cdot \nabla J(\psi_h^{k+1})}{\|\nabla J(\psi_h^k)\|^2}, \\ \rho^k &= \frac{d^k \cdot \nabla J(\psi_h^k)}{\|d^k\|^2}. \end{aligned} \tag{10}$$

Note that the limit membrane energy J is convex for $\Delta p = 0$ in which case the conjugate gradient iterations converge to a global minimum. It is not necessarily convex for $\Delta p \neq 0$, and the nonlinear conjugate gradient may conceivably get trapped at a local minimum.

Even though the method itself is easy to use, the computation of $\nabla J(\psi_h)$ entails some difficulties. Indeed, since QW_0 is a frame-indifferent, isotropic function defined on $\mathbb{M}_{3,2}$ via the singular values of its argument, *viz.* formula (7), the computation of $\frac{\partial(QW_0)}{\partial F}$, which is a 3×2 matrix, requires an adaptation of known results on the differentiation of frame-indifferent, isotropic functions on the space of square matrices \mathbb{M}_n , see [2].

3.3 Computation of the gradient of J

Let $(\lambda_j)_{j=1,\dots,N_h}$ be the components of ψ_h in the shape function basis $(\Theta_j)_{j=1,\dots,N_h}$ of our P_1 or Q_1 finite element space. We clearly have

$$\begin{aligned} \frac{\partial J}{\partial \lambda_j}(\psi_h) &= \int_{\omega} \frac{\partial(QW_0)}{\partial F}(\nabla \psi_h) : \nabla \Theta_j dx_1 dx_2 - \int_{\omega} f \cdot \Theta_j dx_1 dx_2 \\ &\quad - \frac{\Delta p}{3} \int_{\omega} [\lambda_k \lambda_l \det((\partial_1 \Theta_j | \partial_2 \Theta_k | \Theta_l)) + \lambda_i \lambda_l \det((\partial_1 \Theta_i | \partial_2 \Theta_j | \Theta_l)) \\ &\quad \quad + \lambda_i \lambda_k \det((\partial_1 \Theta_i | \partial_2 \Theta_k | \Theta_j))] dx_1 dx_2, \quad j = 1, \dots, N_h, \end{aligned} \quad (11)$$

where $A : B = \text{tr}(A^T B)$ denotes the standard dot product on $\mathbb{M}_{3,2}$.

We compute the 3×2 matrix $\frac{\partial(QW_0)}{\partial F}(\nabla \psi_h)$ via the following lemma.

Lemma 3.2 *The matrix $\frac{\partial(QW_0)}{\partial F}(F)$ has the following explicit form:*

$$\frac{\partial(QW_0)}{\partial F}(F) = R \begin{pmatrix} 0 & 0 \\ \partial_1 \Phi(v_1(F), v_2(F)) & 0 \\ 0 & \partial_2 \Phi(v_1(F), v_2(F)) \end{pmatrix} S, \quad (12)$$

where $(v_1(F), v_2(F))$ are the right singular values of the matrix F , $R \in O(3)$ and $S \in O(2)$ are orthogonal matrices that R^T diagonalizes $FF^T \in \mathbb{M}_3$ and S diagonalizes $F^T F \in \mathbb{M}_2$ both with eigenvalues in increasing order, and Φ is given by formula (7).

Proof. Let us first recall the differentiation result of [2]. Let $Z: \mathbb{M}_n \rightarrow \mathbb{R}$ be a function such that $Z(RFS) = Z(F)$ for all $R, S \in O(n)$. It is known that there exists a symmetric function $\Psi: \mathbb{R}_+^n \rightarrow \mathbb{R}$ such that $Z(F) = \Psi(v_1(F), \dots, v_n(F))$ where $(v_i(F))_{i=1,\dots,n}$ are the singular values of F . In [2], Ball showed that Z is of class C^1 if and only if Ψ is of class C^1 . It is an easy consequence of Ball's results that in this case,

$$\frac{\partial Z}{\partial F}(F) = R \text{diag}(\partial_1 \Psi(v_1(F), \dots, v_n(F)), \dots, \partial_n \Psi(v_1(F), \dots, v_n(F))) S,$$

where $R, S \in O(n)$ are orthogonal matrices occurring in the singular value decomposition of $F = R \operatorname{diag}(v_1(F), \dots, v_n(F))S$ with $0 \leq v_1(F) \leq \dots \leq v_n(F)$. Indeed, for any couple of orthogonal matrices R and S , if we let $Z_{R,S}(F) = Z(RFS)$ and differentiate, we obtain that

$$\frac{\partial Z_{R,S}}{\partial F}(F) = R \frac{\partial Z}{\partial F}(RFS)S = \frac{\partial Z}{\partial F}(F),$$

hence the result by choosing the right orthogonal matrices.

We now recall a few simple facts about the singular value decomposition. By the polar factorization lemma, any $F \in \mathbb{M}_n$ can be written as $F = QU = VQ$, where $U = \sqrt{F^T F}$ and $V = \sqrt{FF^T}$ are symmetric, positive and $Q \in O(n)$. The symmetric matrices U and V are unique, the orthogonal matrix Q is unique if $\det F \neq 0$, it is nonunique otherwise. Let $S \in O(n)$ be such that $U = S^T \operatorname{diag}(v_i(F))S$. Then we have $F = (QS^T) \operatorname{diag}(v_i(F))S$, hence a characterization of the orthogonal matrix S to the right of the singular value decomposition of F as a matrix that diagonalizes $F^T F$. Similarly, the orthogonal matrix R to the left of the singular value decomposition of F is a matrix whose transpose diagonalizes FF^T , and we have the relation $R = QS^T$. Furthermore, we can always choose these matrices in such a way that the singular values are arranged in increasing order.

Let us go back to the case at hand. Let F be a 3×2 matrix. It was established in [7] that $QW_0(F) = QW((F|0))$, where QW is the quasiconvex envelope of the Saint Venant-Kirchhoff energy density itself. Since this energy is left and right invariant by $O(3)$, we also have

$$QW_0(F) = QW((0|F)), \quad (13)$$

Therefore, it follows that the column vectors satisfy

$$\left[\frac{\partial(QW_0)}{\partial F}(F) \right]_{\alpha} = \left[\frac{\partial(QW)}{\partial G}((0|F)) \right]_{(1+\alpha)}, \quad (14)$$

for $\alpha = 1, 2$.

By [7], we have an explicit representation of the quasiconvex envelope of the Saint Venant-Kirchhoff density of the form $QW(z|F) = \Psi(v(z|F))$ with $\Psi: \mathbb{R}_+^3 \rightarrow \mathbb{R}$. Now, by the general result of [2], it follows that

$$\frac{\partial(QW)}{\partial G}((0|F)) = R \operatorname{diag}(\partial_1 \Psi(0, v_1(F), v_2(F)), \dots, \partial_3 \Psi(0, v_1(F), v_2(F))) \bar{S}, \quad (15)$$

where $R^T, \bar{S} \in O(3)$ respectively diagonalize $(0|F)(0|F)^T$ and $(0|F)^T(0|F)$, with the requisite order for the singular values. Now we clearly have

$$(0|F)(0|F)^T = FF^T \text{ and } (0|F)^T(0|F) = \begin{pmatrix} 0 & 0 \\ 0 & F^T F \end{pmatrix}.$$

Therefore, if $S \in O(2)$ diagonalizes $F^T F$ with the eigenvalues in increasing order, it follows that

$$\bar{S} = \left(\begin{array}{c|c} 1 & 0 \\ \hline 0 & S \end{array} \right),$$

since 0 is an eigenvalue of the 3×3 matrix $(0|F)^T(0|F)$.

Now, we just have to identify the last two column vectors in formula (15). This is easy since

$$\begin{aligned} \frac{\partial(QW)}{\partial G} &= R \left(\begin{array}{c|cc} \partial_1 \Psi & 0 & 0 \\ \hline 0 & \partial_2 \Psi & 0 \\ 0 & 0 & \partial_3 \Psi \end{array} \right) \left(\begin{array}{c|c} 1 & 0 \\ \hline 0 & S \end{array} \right) \\ &= R \left(\begin{array}{c|c} \partial_1 \Psi & 0 \\ \hline 0 & \left(\begin{array}{cc} \partial_2 \Psi & 0 \\ 0 & \partial_3 \Psi \end{array} \right) S \end{array} \right) \\ &= R \left(\begin{array}{c|c} \partial_1 \Psi & \left(\begin{array}{cc} 0 & 0 \\ \partial_2 \Psi & 0 \\ 0 & \partial_3 \Psi \end{array} \right) S \end{array} \right). \end{aligned}$$

The conclusion follows from the fact that $\Psi(0, v_1, v_2) = \Phi(v_1, v_2)$ for all $0 \leq v_1 \leq v_2$, see [7]. \square

Remark 2 The expressions of $\partial_1 \Phi(v_1, v_2)$ and $\partial_2 \Phi(v_1, v_2)$ are given by

$$\begin{aligned} \partial_1 \Phi(v_1, v_2) &= \frac{E}{2(1-v^2)} v_1 [v_1^2 + v v_2^2 - (1+v)]_+ \\ &\quad + \frac{E v}{2(1-v^2)(1-2v)} v_1 [v(v_1^2 + v_2^2) - (1+v)]_+ \end{aligned}$$

and

$$\begin{aligned} \partial_2 \Phi(v_1, v_2) &= \frac{E}{2} v_2 [v_2^2 - 1]_+ + \frac{E v}{2(1-v^2)} v_2 [v_1^2 + v v_2^2 - (1+v)]_+ \\ &\quad + \frac{E v}{2(1-v^2)(1-2v)} v_2 [v(v_1^2 + v_2^2) - (1+v)]_+ \end{aligned}$$

for all $0 \leq v_1 \leq v_2$, in view of formula (7). Consequently, to compute the part of the gradient pertaining to QW_0 , we only need to compute the two singular values, which entails solving a second degree equation, and a couple of corresponding orthogonal matrices. \square

4 Numerical tests

Note that in the P_1 case, deformation gradients are constant element-wise. Hence the contributions of QW_0 to the energy and its gradient are computed exactly. However, both dead loading and pressure terms require numerical integration in the P_1 as well as Q_1 cases. In particular, in the Q_1 case, the singular values and orthogonal matrices must be evaluated at Gauss points in each element.

In order to understand the limit model (5) in terms of actual membrane parameters, it should be emphasized that (5) is a rescaled, zero-thickness limit model. In particular, it does not involve the actual nonzero thickness of a given membrane of interest. For instance, the pressure differential Δp stands for the limit of $\varepsilon^{-1}\Delta p_\varepsilon$ when ε goes to zero, where Δp_ε is the actual pressure differential and ε the half-thickness of the membrane. Likewise, body force resultants are rescaled limits.

Now there are infinitely many different ways of embedding an actual nonzero thickness membrane into a family of membranes with vanishing thickness. We can however agree that such a sequence should be made of the same bulk material, hence have material coefficients that are independent of ε , as we have done in the asymptotic analysis. In this context, the computed results for a limit pressure differential Δp of 1.0e+9 as in the first test below, correspond to an actual pressure differential of 50kPa for a 0.1mm thick membrane, and so forth. We will only give the rescaled values below, unless otherwise specified.

Let us first present P_1 tests. The first test (Figure 1) is a circular membrane submitted to an upward pressure differential and clamped on its boundary. A bubble-like deformation is thus created and it is apparent that the live loading character of the pressure is well taken into account, without having to explicitly track the deformed normal vectors.

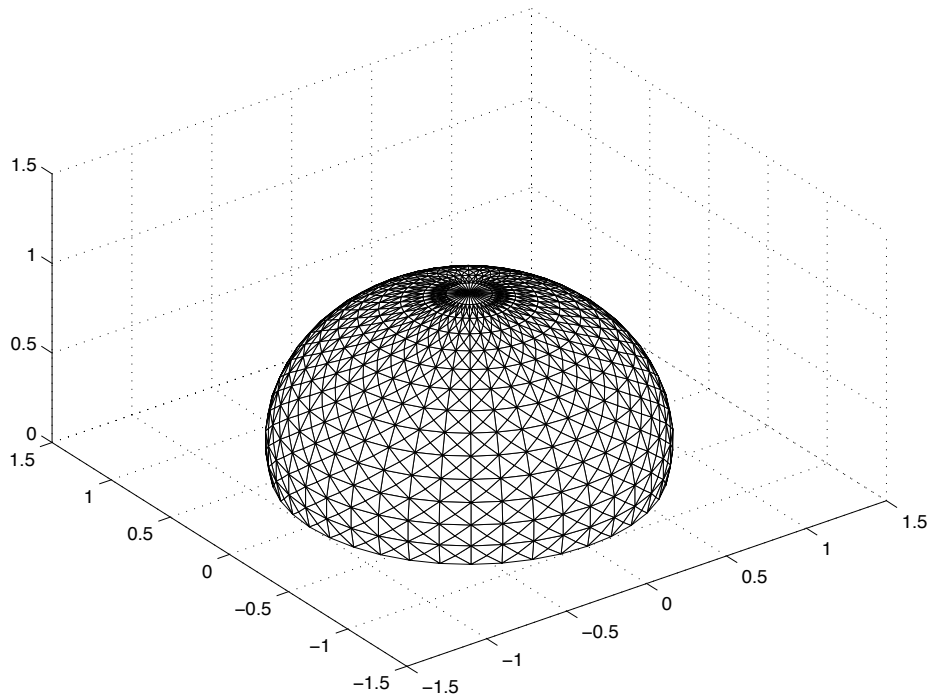


Figure 1. Circular membrane with Young modulus $E = 2.7e+2$ MPa and Poisson ratio $\nu = 0.4$, corresponding to an elastomer, (rescaled) pressure differential $\Delta p = 1.0$ GPa, zero dead loading body force.

Our second P_1 test is an airbag: a pillow-like structure submitted to an outward pressure differential that inflates it. To compute it, we use two equal square reference domains corresponding to the upper and lower parts of the airbag, with the condition that horizontal displacements agree and vertical displacements vanish on their common boundary.

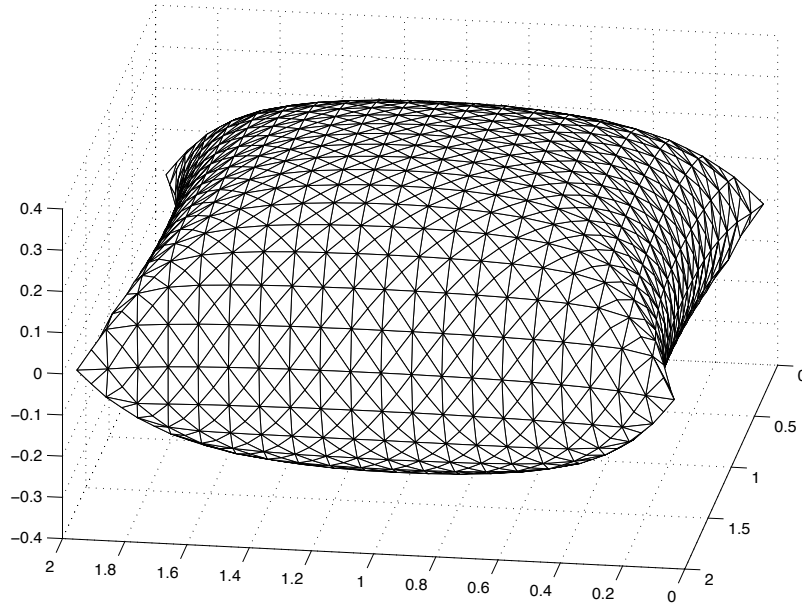


Figure 2. P_1 airbag, same values except pressure differential $\Delta p = 1.0e+7$.

It is instructive to compare this test with the corresponding one in [12]. Because of the relaxed nature of the membrane energy we use, there is no need for a special treatment of the areas located near the middle of the airbag sides, where wrinkling occurs. Such wrinkling is smoothed out by the Γ -limit process, as a result of weak convergence. On the other hand, we do not capture wrinkle details. However, our model can predict wrinkled areas which correspond to areas where the deformation gradient lies in the subset of $\mathbb{M}_{3,2}$ in which the energy is relaxed. See [6] for a description of this subset in terms of the singular values of the deformation gradient.

Let us now show the results of a few Q_1 tests. First is the same airbag as before.

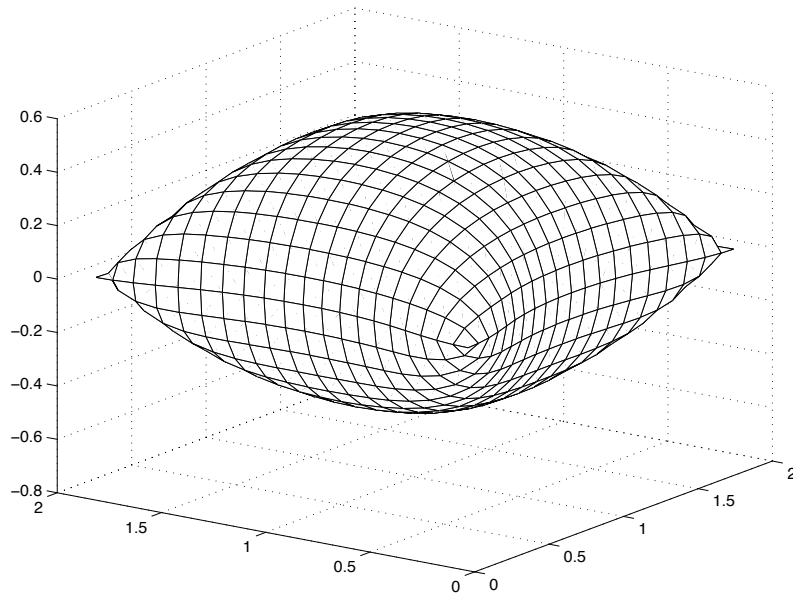


Figure 3. Q_1 airbag.

We next compute again the same airbag, with an added point force $f_1 = f_2 = 0$ and $f_3 = -1.0e+9$, slightly off-center on the top surface.

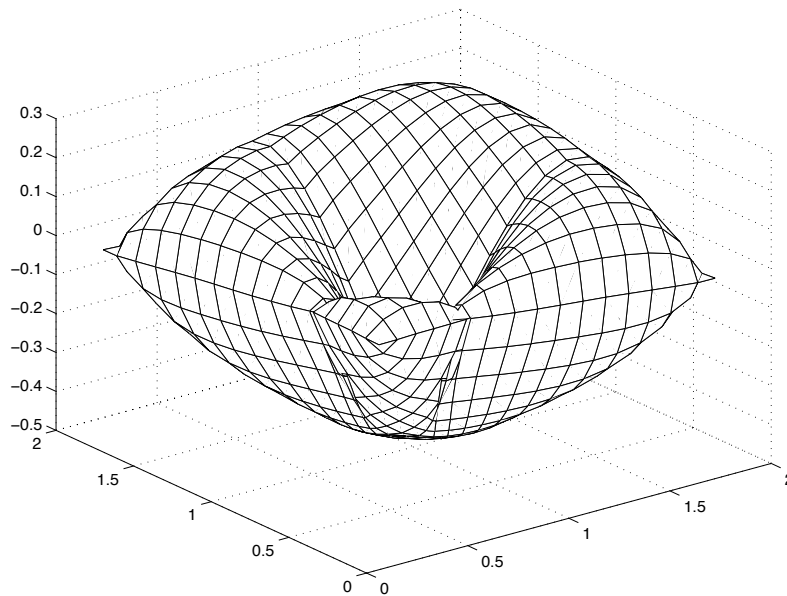


Figure 4. Q_1 airbag with point force.

Back to P_1 -tests, a square membrane attached by its four corners and submitted to a vertical point force applied at the center.

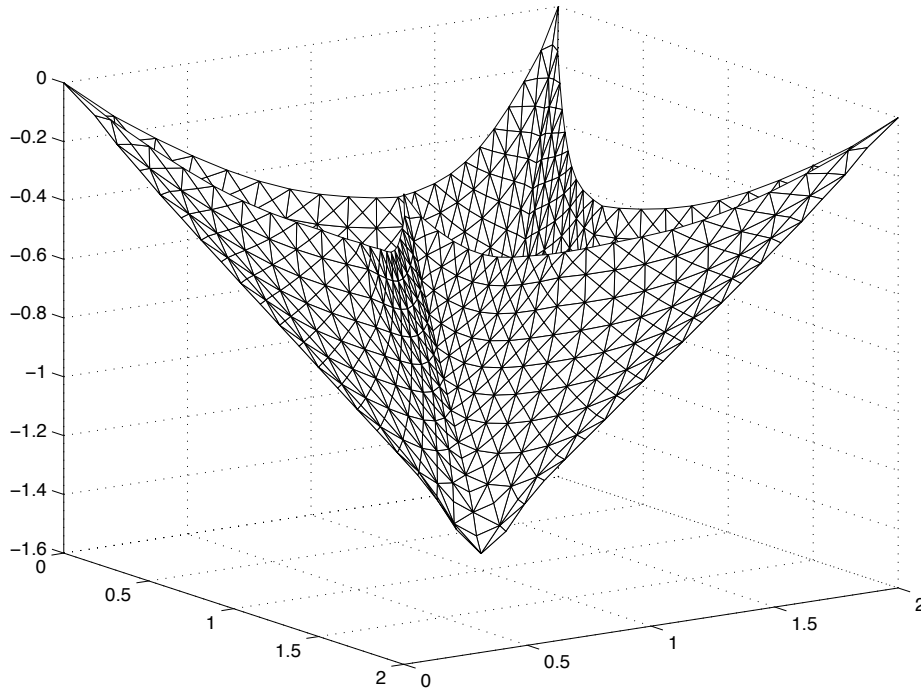


Figure 5. Square membrane, with $E = 2.1\text{e}+8$, $\nu = 0.25$ and central point force $f_1 = f_2 = 0$ and $f_3 = -1.0\text{e}+10$.

Our next tests are in the context of the modeling of fabrics. We take values for the Young modulus $E = 2,500$ Pa and Poisson ratio $\nu = 0.01$ that are characteristic of cotton fabric, see [4]. These values are rescaled with respect to the thickness since the bulk Young modulus of cotton is of the order of 8 GPa.

In Figure 6, we consider a square piece of fabric attached at its center and submitted to a vertical dead loading body force $f_3 = -1,000$, slightly counterbalanced by an upward pressure differential $\Delta p = 100$. The lateral sides are hanging free.

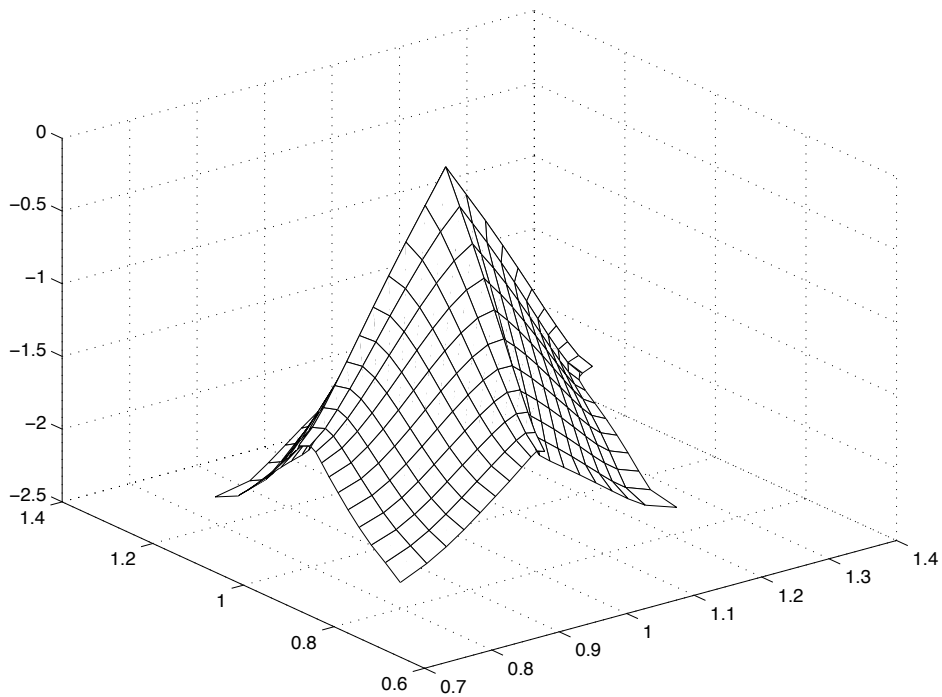


Figure 6. Q_1 square piece of fabric.

Our last test is a tablecloth. The material constants and applied forces are the same as above, and the displacement is set to zero on the center square that represents the table, *i.e.*, the fabric is not allowed to slide across the table like an actual tablecloth.

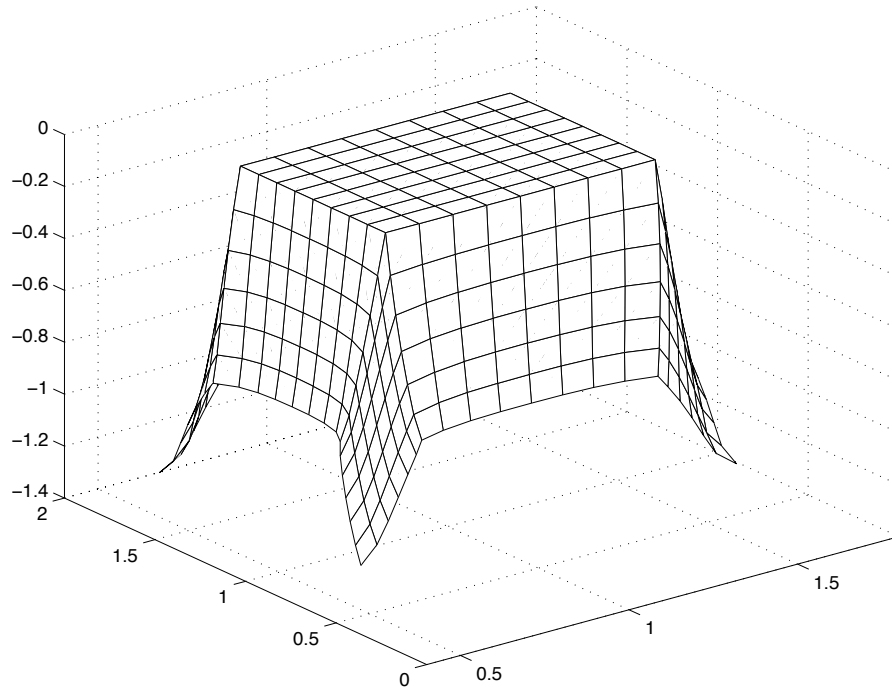


Figure 7. Q_1 tablecloth.

References

- [1] J.M. Ball, Convexity conditions and existence theorems in nonlinear elasticity, *Arch. Rational Mech. Anal.*, 63, 1977, 337–403.
- [2] J.M. Ball, Differentiability properties of symmetric and isotropic functions, *Duke Math. J.*, 51, 1984, 699–728.
- [3] B. Dacorogna, *Direct Methods in the Calculus of Variations*, Applied Mathematical Sciences, 78, Springer-Verlag, Berlin, 1989.
- [4] T.J. Kang and W.R. Yu, Drape simulation of woven fabric using finite-element method. *J. Text. Inst.*, 86, 1995, 635–648.
- [5] N. Kerdid, H. Le Dret and A. Saïdi, Approximation numérique d’un problème de membrane non linéaire, *C. R. Acad. Sci. Paris, Série I*, 340, 2005, 69–74.

- [6] H. Le Dret and A. Raoult, The nonlinear membrane model as variational limit of three-dimensional nonlinear elasticity, *J. Math. Pures Appl.*, 75, 1995, 551–580.
- [7] H. Le Dret and A. Raoult, The quasiconvex envelope of the Saint Venant-Kirchhoff stored energy function, *Proc. Roy. Soc. Edinburgh A*, 125, 1995, 1179–1192.
- [8] H. Le Dret and A. Raoult, Quasiconvex envelopes of stored energy densities that are convex with respect to the strain tensor, in *Calculus of variations, applications and computation, Pont-à-Mousson 1994*, (C. Bandle, J. Bemelmans, M. Chipot, J. Saint Jean Paulin, I. Shafrir eds), Pitman Research Notes in Mathematics, Longman, 1995, 138–146.
- [9] H. Le Dret and A. Raoult, The membrane shell model in nonlinear elasticity: A variational asymptotic derivation, *J. Nonlinear Sci.* Vol.6, 1996, 59–84.
- [10] A. Saïdi, Analyse mathématique et numérique de modèles de structures intelligentes et de leur contrôle, Doctoral Dissertation, Université Pierre et Marie Curie (Paris 6), 1997.
- [11] A. Saïdi, Finite element approximation and optimization of smart structures, to appear.
- [12] M. Stanuszek, FE analysis of large deformations of membranes with wrinkling, *Finite Elements in Analysis and Design* 39, 2003, 599–618.